

Supplemental Information



Movie S1, related to Figure 1. SOP pattern development. Notum genotype: shotgun:GFP, neuron GAL4, UASn GMCA. Anterior to the right. Scale bar, 50μm. Timelapse (upper left, hh:mm), 1 frame = 30 minutes.

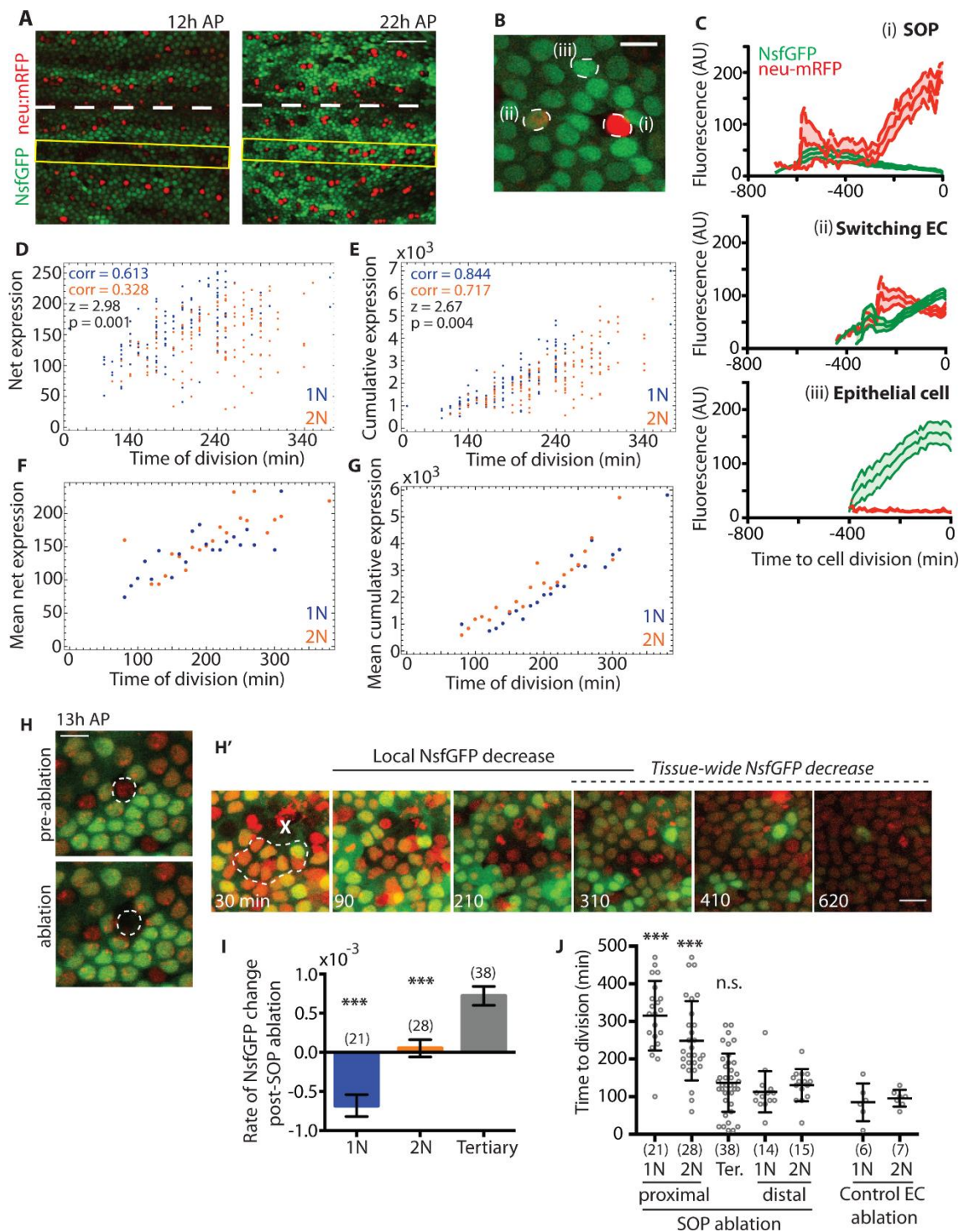


Figure S1, related to Figure 2. (A) Notum expressing N^{sfGFP} (green) indicating Notch response and neu-mRFP (red) indicating pro-neural gene expression at 12 and 22h AP. Dashed line indicates midline. Yellow box highlights bristle row 2. Unless otherwise indicated, N^{sfGFP} measurements were made for developing SOP neighbourhoods in row 2. Scale bar, 50µm. (B) N^{sfGFP} and neu-mRFP expressing notum cells, indicating cells expressing (i) only pro-neural reporter, (ii) both reporters, or (iii) only Notch reporter. Scale bar, 10µm. (C, i-iii) Corresponding N^{sfGFP} and neu-mRFP dynamics in (i) SOP cells (n = 7, N = 2), (ii) cells expressing both reporters (n = 35, N = 3), and (iii) epithelial cells (n = 6, N = 1). Mean ± SEM. (D, E) Plot of individual data points corresponding to net (D) or cumulative (E) NsfGFP expression. (F) Mean net N^{sfGFP} levels at the time of division increases with time of division. (G) Mean cumulative N^{sfGFP} expression increases with time of division. (D-G) n=266 cells, N=3 nota; corr = Pearson's correlation coefficient, z-value = Fisher r-to-z transformation, p-value = one-tailed test, 1N>2N. (H) Notum expressing N^{sfGFP} (green) indicating Notch response and ubi-H2B-mRFP (red) indicating nuclei 13h AP. Pre-ablation and post-ablation panels, targeted SOP cell is outlined. In pre-ablation image, the indicated SOP is the only SOP in the panel. Scale bar, 10µm. (H') Example of post-ablation tissue (from region in H). White dashed line indicates cells that are primary and secondary neighbours to the ablated SOP cell (marked with X). Local NsfGFP decrease precedes tissue-wide NsfGFP decrease, suggesting that loss of SOP leads to acute loss of Notch response. Cell division occurs (*e.g.*, see panel at 310 min) and epithelium heals. (I) Rate of change of normalized NsfGFP fluorescence in ECs neighbouring an ablated SOP cell as in (H'). 1N, primary neighbour to ablated SOP; 2N, secondary neighbour to ablated SOP; tertiary, cells 2N+ to ablated SOP,

but $\leq 2N$ to an nearby, intact, SOP. Data generated from a total 5 ablations performed across 3 pupae, (n) = number of cells. Rate measured from onset of timelapse imaging, beginning 30 min after ablation, $\sim 13.5h$ APF. *** $p \leq 0.001$, One-way ANOVA, multiple comparisons, comparing to tertiary cells. Mean \pm S.D. shown. (J) Cell division is delayed following SOP ablation. 1N, proximal: primary neighbour to ablated SOP; 2N, proximal: secondary neighbour to ablated SOP; ter.: tertiary cells as defined in (I); 1N, distal: primary neighbours to an intact SOP in same notum as proximal cells, but $>100 \mu m$ away (as a developmental timing control); 2N, distal: secondary neighbors to an intact SOP in the same notum as proximal cells, but $>100 \mu m$ away; 1N, control EC ablation: primary neighbor to an ablated EC (SOPs intact, as a wounding control); 2N, control EC ablation: secondary neighbor to an ablated EC (SOPs intact). Two control EC ablations were performed in one pupae. (n) = number of cells. T = 0 at $\sim 13.5h$ AP. Mean \pm S.D. shown. *** $p \leq 0.001$, by One-way ANOVA, multiple comparisons, comparing to tertiary cells. N.s., by one-way ANOVA using control 1N groups.

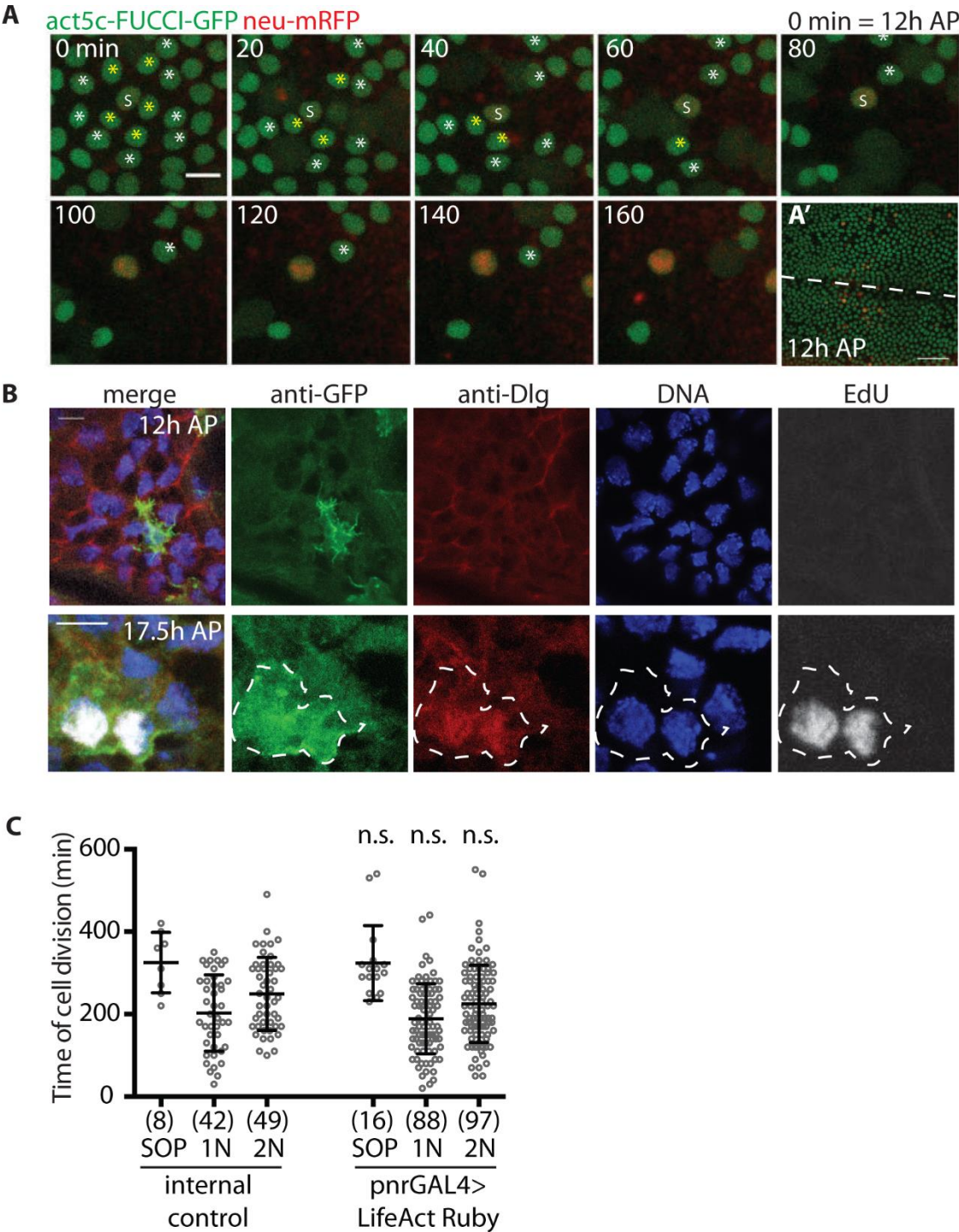


Figure S2, related to Figure 3. (A) act-FUCCI-GFP (green) and neu-mRFP (red). Loss of GFP signal indicates G2-exit. S, SOP cell; yellow asterisk, 1N; white asterisk, 2N. Scale bar, 10 μm . (A') Zoomed out image of full FUCCI-GFP expressing nota; scale bar, 50 μm , dashed line indicates midline. All cells are in G2. (B) 12h (upper panels) and 17.5h (lower panels) AP nota labeled with EdU to indicate absence of ECs in S-phase; cell cycle progression in SOP cell lineage serves as a control. Genotype: neu-GAL4, UAS-GMCA; thus anti-GFP panels visualize GMCA/F-actin in SOP or SOP daughter (pIIa/pIIb) cells. Dashed white line outlines pIIa/pIIb cell bodies. Scale bar, 5 μm . (C) Cell division timing in shotgun^{GFP}, neu-GMCA; pnrGAL4 > UAS-LifeActRuby control pupae (N=2, n = as noted). N.s., not significant by unpaired t-test, compared by cell type (i.e., 1N inside vs 1N outside). Cells counted outside pnr domain as internal control to inside pnr domain UAS expressing cells.

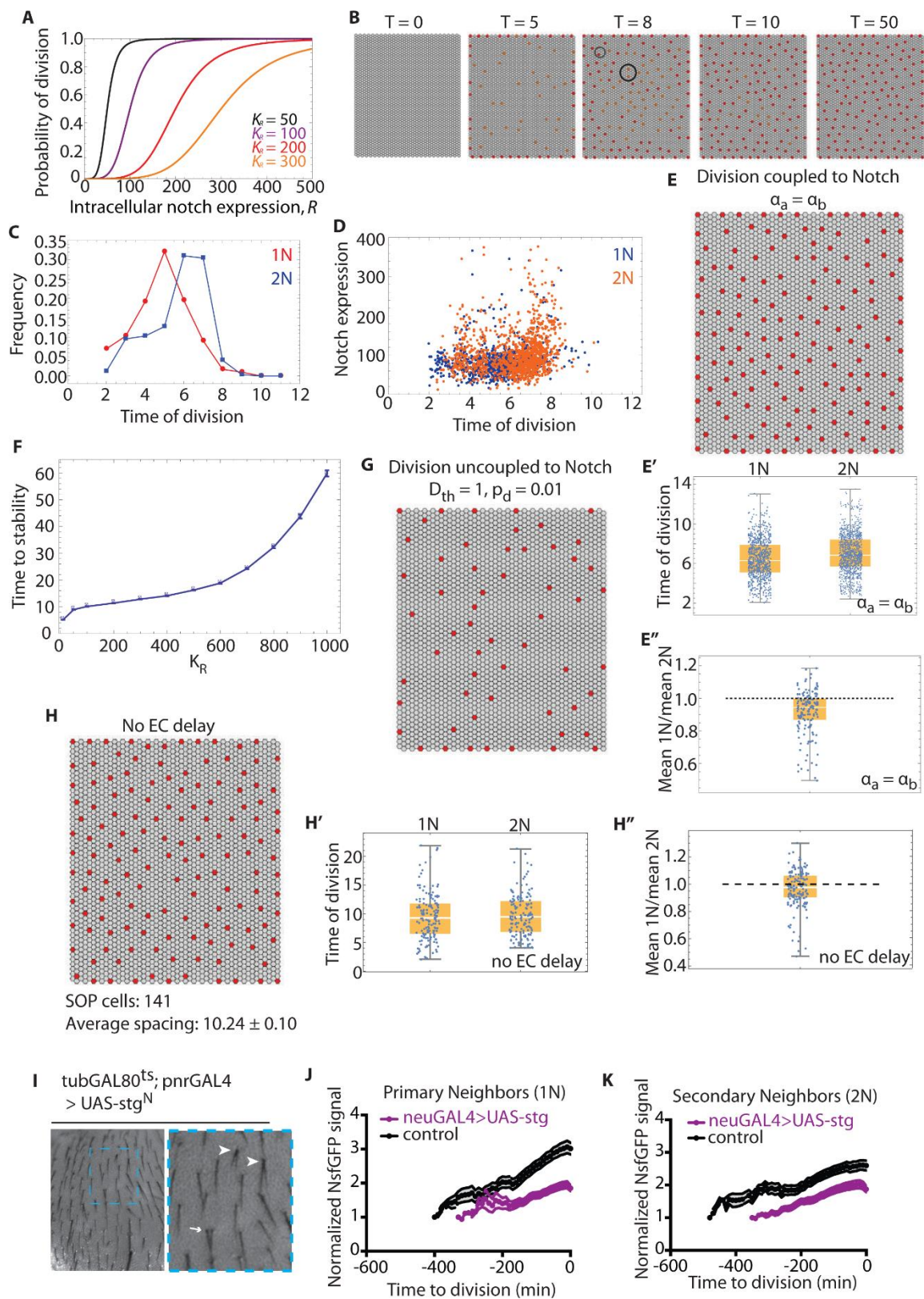


Figure S3, related to Figure 4. (A) Probability of division for given values of K_R and $q=5$. (B) Time course of 'wildtype' pattern, $R_{th} = 200$, $p_d = 0.5$. Red cells = high Delta; Orange cells = intermediate; Uncolored/gray = high Notch. Circles indicate local, transient pattern disruptions that are resolved. (C) Frequency of divisions for the wildtype model by time-step. (D) Level of Notch expression (AU) at division time for dividing cells in the wildtype model. (E) Model output when cell division is coupled to Notch but $\alpha_a = \alpha_b$. (E') Timing of 1N and 2N cell divisions when $\alpha_a = \alpha_b$. (E'') Local ratio of mean 1N and mean 2N time of divisions when $\alpha_a = \alpha_b$. (F) Time to stability for given values of R_{th} . Stability is defined as >2 AU of time without cell fate changes in the pattern. (G) Final time point for simulations where cell division is uncoupled from Notch signaling for D_{th} and p_d indicated. (H) Model output when cell division is coupled to Notch but independent of protrusion length, with $\alpha_a = 0$, $\alpha_b = 1.2$ (thus 1N and 2N ECs have equivalent incoming Notch signal; there is no delay between mean 1N and mean 2N division time) (H') Timing of 1N and 2N cell divisions and (H'') local ratio of mean 1N and mean 2N time of divisions for simulation as in (H). (I) Adult dorsal thorax microchaete patterns of the genotypes indicated. Anterior to the top of each panel. Arrowheads indicate split microchaete; arrow indicates 'twin' adjacent microchaete. (J) N^{sfGFP} signal dynamics in wild type primary or (K) secondary ECs neighbouring SOPs overexpressing *cdc25/string* (*stg*) under *neu-GAL4* (purple; $n=28$, $N=3$) or control SOPs (black; *neuGAL4*, *UAS-lifeActRuby*; $n=30$, $N=3$). Mean \pm SEM shown.

Supplemental Experimental Procedures

Fly strains. Drivers: tub-GAL80^{ts}/CyO; neuralized-GAL4, UAS-GMCA/TM6B

neu-GAL4, UAS-GMCA/TM6B

shotgun^{GFP}; neu-GAL4, UAS-GMCA/TM6B

shotgun^{GFP}, neu-GMCA/CyO-GFP; pnr-GAL4/TM6B

N^{sfGFP}/CyO-GFP; pnr-GAL4/TM6B

N^{sfGFP}/CyO-GFP; neu-GAL4/TM6B

Responders: UAS-wee1RNAi; UAS-myt1RNAi; UAS-stg RNAi; UAS-Su(H) RNAi;

UAS-lifeActRuby; UAS-string^N.

Other: N^{sfGFP}; act-FUCCI-GFP; neuralized-nls:mRFP

Immunofluorescence. Nota were fixed in 4% formaldehyde / 1x PBS (Sigma) and washed to permeabilize with 1x PBS with 0.01% Triton X-100 (1x PBST). Samples were blocked (50% blocking buffer: 3% FBS, 5% BSA in 1x PBS) for 1h at room temperature. Primary antibodies (anti-Discs-large, DSHB 4F3, Parnas et al., Neuron 2001; anti-GFP, AbCam, ab#13970) were added to 5% blocking buffer in 1x PBST to concentrations listed, and incubated overnight at 4°C. Samples were washed several times with 1x PBST, and incubated in secondary antibody in 1x PBST at room temperature for 2-4 h. Where needed, nota were further incubated for 20 min at room temperature with phalloidin (Acti-stain 555 phalloidin, Cytoskeleton PHDH1-A, 1:500) and DAPI (Molecular Probes D1306, 1:1000) or Hoechst33342 (provided with Clk-it EdU kit, ThermoFisher C10340, 1:2000). Final washes in 1x PBST were followed by overnight equilibration in mounting media (50% glycerol/1x PBS).

Mathematical Methods in Full

Protein dynamics

We used a mathematical model to simulate lateral inhibition by Delta-Notch signalling. The model is defined by a set of coupled differential equations (based on (S1)), which describe the dynamics of Notch (N_i), Delta (D_i) and a Reporter of Notch signalling (R_i) for individual cells:

$$\frac{dN_i}{dt} = \beta_N - \frac{N_i D_{trans}}{k_t} - \frac{N_i D_i}{k_c} - \gamma_N N_i \quad (1)$$

$$\frac{dD_i}{dt} = \beta_D \frac{1}{1 + R^m} - \frac{N_i D_{trans}}{k_t} - \frac{N_i D_i}{k_c} - \gamma_D D_i \quad (2)$$

$$\frac{dR_i}{dt} = \beta_R \frac{(N_i D_{trans})^s}{k_{RS} + (N_i D_{trans})^s} - \gamma_R R_i \quad (3)$$

The parameters β_N , β_D , β_R and γ_N , γ_D , γ_R are the production and degradation rates of Notch, Delta and the Reporter of Notch signalling respectively. The constants k_t and k_c determine the strength of Delta-Notch interactions in trans and in cis respectively, and k_{RS} is the dissociation constant for the intracellular signal. D_{trans} and N_{trans} indicate the incoming Delta and Notch signal and are determined by summing the signal from all contacting cells, scaled by a factor α_a and α_b for apical and basal contacts respectively. We normalized these values so that $\alpha_a = 1$ and $\alpha_b = 0.2$. These relative weights for apical and basal signalling are in agreement with previously measured values, although our model is relatively robust to changes in α_b (S2). A Gaussian noise term was applied to initiate protein concentrations and to the concentrations at each time step.

Protrusion dynamics

Basal protrusions were implemented as 2D circular areas, extending from the centre of each cell. Radii were drawn from a normal distribution with mean $F_{mean} = 5.6$ (2.3 times the cell diameter) and variance 0.3 (S2). A contact probability term was introduced to account for the angular directions of protrusions that were observed and hence the associated likelihood of two protrusions signalling to each other at different ranges. This was implemented in the model by assigning each cell a randomly selected ‘direction’ term, r , an integer between 1 and 100. For any two cells ($cell_1$ and $cell_2$) spaced a distance, d , such that their protrusions are of sufficient length to signal, a signal occurs if the condition is met such that:

$|vertr_{Cell_1} - r_{Cell_2}| < \frac{P}{d^2}$, where P was a constant variable. Hence the likelihood of a contact being made

reduced in proportion to the square of the distance between two cells. At each time step a random number generator was used to determine whether the protrusions of a particular cell (i.e. the length and directionality of the protrusion) would be updated. Thus, protrusion lifetimes were set according to a Poisson distribution.

Cell division

We model cell division in wild-type flies by assuming that *cdc25* activity is coupled to the expression of the intracellular Notch reporter, R . The cumulative expression of R at division scales linearly with the division time in control experiments, whereas the value of R itself appears to fluctuate within a confined window (Fig. 3). These data suggest that cells respond to the absolute, rather than cumulative, signal expression, and divide with a probability that is a function of their intracellular Notch expression. To model cell division in this manner, we define,

$$p_d = \frac{R^q}{K_R^q + R^q} \quad (4)$$

where p_d is the probability that a cell divides within a each time step in our simulations, K_R is the hill function dissociation constant and determined the range of values of R for which division is likely. We note that a similar set-up where *cdc25* was coupled to the cumulative expression of the Notch reporter gave similar results (not shown). Cells that have divided maintain their expression levels prior to division but no longer participate in lateral signalling so that they are excluded from the calculation of N_{trans} and D_{trans} for other cells. Also note that we set a threshold in the simulation time t_{th} below which cells cannot enter division. This is important in the model because the early dynamics of Delta-Notch are so that most cells go through transient phases where they express both proteins and we want to avoid division at that stage (S3).

Simulation Parameters

The same baseline parameters used for all simulations: $\beta_N = 100$, $\beta_D = 500$, $\beta_R = 300000$, $\gamma_N = \gamma_D = \gamma_R = 1$, $k_t = k_c = 1$, $k_{RS} = 10000000$, $m = 2$, $s = 2$, $q = 5$, $F_{mean} = 5.6$, $F_{se} = 0.3$, $F_{rate} = 10$, $error = 0.01$, $\alpha_a = 1$, $\alpha_b = 0.2$, $P = 1000$ and $t_{th} = 2$. Initial expression values were sampled from a Normal distribution $N(10^{-3}\beta_N, 10^{-4}\beta_N)$ and $N(10^{-3}\beta_D, 10^{-4}\beta_D)$ for Notch and Delta respectively. All R values were initially set to 0. The cell radius was set equal to 2. We varied the division rule (e.g. dependence on

Delta or intracellular Notch expression), in individual simulations as summarized in each figure legend.

The model was applied to a uniform hexagonally packed 2D array of 50x50 cells. Simulations were performed by numerically solving equations (1)-(3) using the Euler method. The Euler step was set to 0.005 and all simulations were run until stability was reached (defined as no changes in cell fate for 2a.u. of time), which was within $T=40$ a.u. in simulation time.

Supplemental References

[S1]. Sprinzak D, Lakhanpal A, LeBon L, Garcia-Ojalvo J, Elowitz MB. Mutual Inactivation of Notch Receptors and Ligands Facilitates Developmental Patterning. PLoS Comput Biol. 2011 7(6):e1002069.

[S2]. Cohen M, Georgiou M, Stevenson NL, Miodownik M, Baum B. Dynamic filopodia transmit intermittent Delta-Notch signaling to drive pattern refinement during lateral inhibition. Dev Cell. 2010 Jul 20 19(1):78-89.

[S3]. Collier JR, Monk N a, Maini PK, Lewis JH. Pattern formation by lateral inhibition with feedback: a mathematical model of delta-Notch intercellular signalling. J Theor Biol. 1996 183(4):429-46.